nature communications

Article

https://doi.org/10.1038/s41467-024-51852-2

Near surface oxidation of elemental mercury leads to mercury exposure in the Arctic Ocean biota

Received: 15 January 2024

Accepted: 20 August 2024

Published online: 31 August 2024

Check for updates

Seung Hyeon Lim[1], Younggwang Kim[1], Laura C. Motta[2], Eun Jin Yang[3], Tae Siek Rhee[3], Jong Kuk Hong[3], Seunghee Han[4] & Sae Yun Kwon[1]

Atmospheric mercury (Hg(0), Hg(II)) and riverine exported Hg (Hg(II)) are proposed as important Hg sources to the Arctic Ocean. As plankton cannot passively uptake Hg(0), gaseous Hg(0) has to be oxidized to be bioavailable. Here, we measured Hg isotope ratios in zooplankton, Arctic cod, total gaseous Hg, sediment, seawater, and snowpack from the Bering Strait, the Chukchi Sea, and the Beaufort Sea. The Δ^{200}Hg, used to differentiate between Hg(0) and Hg(II), shows, on average, 70% of Hg(0) in all biota and differs with seawater Δ^{200}Hg (Hg(II)). Since Δ^{200}Hg anomalies occur via tropospheric Hg(0) oxidation, we propose that near-surface Hg(0) oxidation via terrestrial vegetation, coastally evaded halogens, and sea salt aerosols, which preserve Δ^{200}Hg of Hg(0) upon oxidation, supply bioavailable Hg(II) pools in seawater. Our study highlights sources and pathways in which Hg(0) poses potential ecological risks to the Arctic Ocean biota.

Mercury (Hg) is a globally distributed trace metal, which is mainly present in the atmosphere as gaseous elemental Hg (Hg(0))[1]. When Hg(0) is oxidized in the atmosphere, Hg(II) deposits to the biosphere via wet (precipitation) and dry deposition (particulate bound Hg; PBM)[2]. While the majority of anthropogenic Hg emissions occur in the mid-latitudes in industrialized regions of Asia and North America[3], the long-range transport of Hg(0) and accelerated effects of global warming pose significant Hg threats to remote polar regions such as the Arctic. A recent estimate has suggested that atmospheric Hg deposition, derived from long-range transport, mounts to 65 ± 20 Mg yr^{-1} in the Arctic Ocean[4]. Ocean currents (55 ± 7 Mg yr^{-1})[5] and continental export from rivers (41 ± 4 Mg yr^{-1})[6–8] and coastal erosion (39 ± 30 Mg yr^{-1}) also supply substantial amounts of Hg[4]. Owing to the volatile nature, Hg(0) re-emission into the atmosphere is anticipated to change upon surface warming[9,10], decline in sea ice cover[9,11], and via intensified wildfire events[9,12].

There are substantial gaps in knowledge regarding the sources and environmental pathways governing Hg exposure to the Arctic biota, despite the elevated Hg concentrations frequently reported in the tissues of marine mammals[13,14]. In many remote oceans other than the Arctic, it has been suggested Hg(II) deposited from the atmosphere[15,16] and Hg(II) introduced via continental export[17] are subjected to microbial methylation in the deep water column[18,19] and aquatic sediment[20]. Given the bioaccumulative nature, the resultant methylmercury (MeHg) biomagnifies through the aquatic food web. In the Arctic Ocean, it is possible that certain biogeochemical features and/or seasonal events enhance ecological Hg exposure. In addition to high surface seawater Hg level[21], microbial and abiotic methylation are thought to take place both in the (sub)surface[22–24] and deeper water columns in the Arctic Ocean[25,26]. Seasonally important events such as the Atmospheric Mercury Depletion Event (AMDE), mediated by coastally evaded halogen[27], and spring freshet also cause substantial Hg deposition and releases along with increased primary productivity[24]. It is unclear, however, whether these features/events fully explain Hg levels found in marine mammals and health risks posed to the Arctic populations, who regularly harvest and consume marine products[28]. It is estimated that 63% of the Arctic Inuit

[1]Division of Environmental Science and Engineering, Pohang University of Science and Technology, 77 Cheongam-Ro, Nam-Gu, Pohang 37673, Republic of Korea. [2]Marine Chemistry & Geochemistry, Woods Hole Oceanographic Institution, 266 Woods Hole Road, Woods Hole, MA 02543, USA. [3]Korea Polar Research Institute, Incheon 21990, Republic of Korea. [4]School of Earth Sciences and Environmental Engineering, Gwangju Institute of Science and Technology (GIST), Gwangju 61005, Republic of Korea. e-mail: saeyunk@postech.ac.kr

population is subjected to food insecurity, which is much higher than the global estimates of food insecurity (9.2%)[28]. In the absence of local anthropogenic activities, the sources and pathways leading to spatially unequal Hg exposure and health risks posed to the Arctic biota and populations should be explored.

Hg stable isotopes have played an instrumental role in deciphering sources and processes governing Hg exposure in aquatic ecosystems. Given the absence of isotopic changes during bioaccumulation and trophic transfer[29,30], mass-dependent (MDF; δ^{202}Hg) and mass-independent Hg isotope fractionation signatures (MIF; Δ^{199}Hg, Δ^{200}Hg, Δ^{201}Hg, Δ^{204}Hg) of biota have provided multi-dimensional information regarding sources, chemical forms of Hg, and biogeochemical processes prior to exposure[31]. Among numerous applications in the Arctic[8,32–42], Jiskra and co-workers[43] recently employed Δ^{200}Hg to model the relative Hg(0) and Hg(II) input to the global seawater. The Δ^{200}Hg has been used as a tracer for atmospheric Hg(0) and Hg(II) deposition given that Δ^{200}Hg anomalies occur exclusively via tropospheric oxidation, resulting in a positive Δ^{200}Hg in Hg(II) and a negative to near-zero Δ^{200}Hg in Hg(0)[44]. The model estimated that, in the Arctic, 70% of gross Hg input occurs via atmospheric gaseous Hg(0) dissolution into seawater relative to wet/dry Hg(II) deposition, leaving near-zero Δ^{200}Hg in both the seawater and biota. Dissolution and evasion of Hg(0) from seawater, resulting in bi-directional gas exchange of Hg(0), has previously been measured in various oceanic basins[45–47]. Given the active Hg redox cycle in polar marine waters[11,48] and the preferential assimilation of dissolved Hg(II) by plankton[49–51], the oxidation of gaseous Hg(0) in seawater followed by passive Hg(II) diffusion into the plankton cell may explain the near-zero Δ^{200}Hg in the Arctic Ocean seawater and biota. Alternatively, other sources or processes may be responsible for supplying bioavailable Hg(II) pools in the seawater.

We measured total Hg (THg) concentration and Hg isotope ratios in zooplankton, Arctic cods (*Boreogadus saida*), and other environmental matrices (total gaseous Hg; TGM, seawater, precipitation, sediment, snowpack) sampled from the Bering Strait (Section A), Chukchi Sea (Section B), and Beaufort Sea (Section C) (Fig. 1, Supplementary Fig. 1). Given that our sampling sites vary in their distances away from land and major riverine basins, we compiled Hg isotope data reported previously from the Mackenzie River[38]. The sampling was performed during non-AMDE season to exclude the influence of unique seasonal events on ecological Hg exposure. This study aims to quantify potentially widespread Hg(0) influence in biota and environmental matrices of the Arctic Ocean and assess pathways in which Hg(0) is oxidized to become bioavailable. Our results would enable a greater understanding towards sources and exposure pathways of Hg to the Arctic Ocean food web.

Results and discussion

Overall Hg pattern in the Arctic Ocean

In the Beaufort Sea, where diverse environmental media were sampled (Section C, Fig. 1b), we observed an average TGM and precipitation THg of 1.38 ± 0.27 ng m^{-3} (n = 3; 1 SD) and 3.03 ng L^{-1} (n = 1), respectively. The seawater THg (0.38 ± 0.15 ng L^{-1}; 1.89 ± 0.72 pM; n = 13) shows no significant relationship with distance (regression; p = 0.48), while the surface sediment THg (62.9 ± 14.4 ng g^{-1}, n = 11) increase with increasing distances away from the Mackenzie River to the Beaufort Sea (Supplementary Fig. 2; regression; p < 0.05). In the Chukchi Sea (Section B), the snowpack sampled on sea ice have THg concentrations (1.44 ± 0.42 ng L^{-1}, n = 3) lower than that of AMDE-affected snowpack (104 ± 40.5 ng L^{-1})[52]. The Arctic cods display a wide THg range of 48.5 to 118 ng g^{-1} (n = 3) due to their varying body length (6.2–14.5 cm). The observed THg are within the range of THg of Arctic cod (85 ± 5 ng g g^{-1} to 190 ± 30 ng g g^{-1})[53–55] sampled at similar locations.

The zooplankton sampled across the Arctic Ocean display notable THg and MeHg patterns with respective to their size fractions (0.2–1 mm, 1–5 mm, >5 mm), sampled locations, and distances away from land. The average THg are ranked in the order of medium (64.0 ± 48.4 ng g^{-1}, 1 SD, n = 19) > small (62.2 ± 37.3 ng g^{-1}, n = 14) > large size fractions (35.1 ± 26.3 ng g^{-1}, n = 11), with no significant difference between small and medium size fractions (Mann–Whitney test; p = 0.87). The observed THg are within the ranges of zooplankton previously measured from the Chukchi Sea (42.0 ± 2.0 ng g^{-1}) and the Beaufort Sea (68.0 ± 6.6 ng g^{-1})[56]. The % MeHg, measured in a subset of zooplankton, increase with size fractions at their individual sampled locations (Section A; 0.05 to 5%, Section C; <2 to >7%) (Source Data),

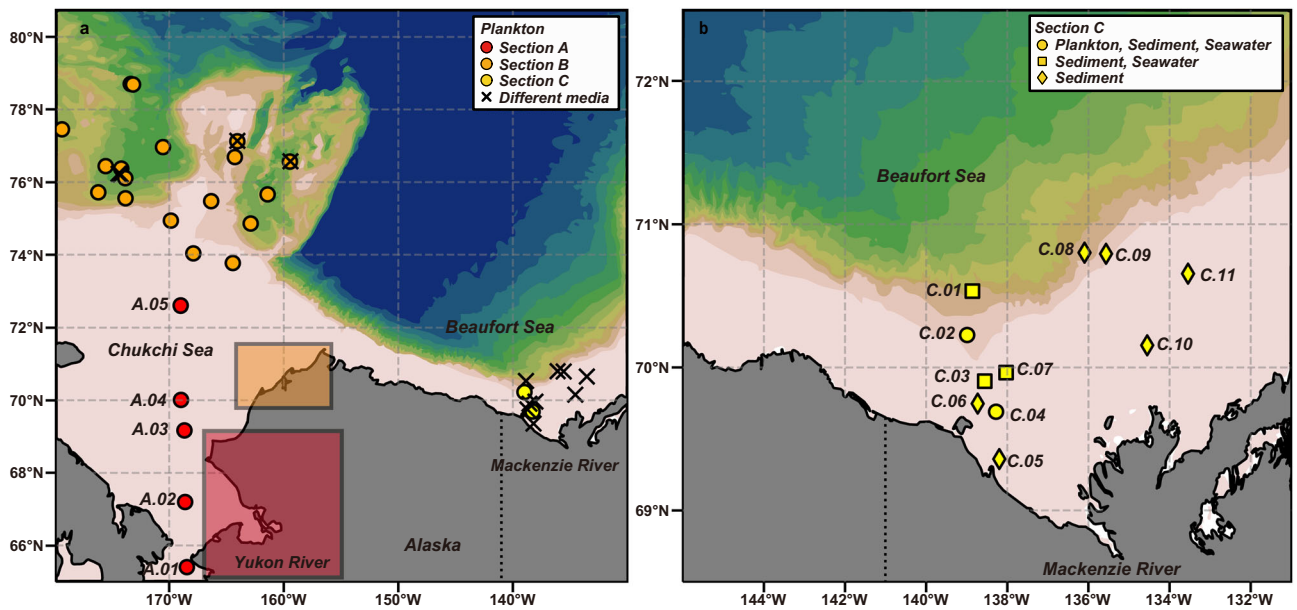

Fig. 1 | Map of the sampling locations. a Zooplankton collection sites at Section A (the Bering Strait to the Chukchi Sea) and zooplankton, Arctic cod, and snowpack collection sites at Section B (the Chukchi Sea). Red and orange boxes indicate sampling locations of beluga whale (*Delphinapterus leucas*), ringed seal (*Pusa hispida*) and polar bear (*Ursus maritimus*) from Masbou et al.[34], respectively. **b** Zooplankton and environmental matrices (sediment, seawater, TGM, precipitation) sampled at Section C (the Mackenzie River estuaries to the Beaufort Sea). Source data are provided as a Source Data file. Figures were prepared using the dataset sourced from The GEBCO Grid[109].

https://doi.org/10.1038/s41467-024-51852-2

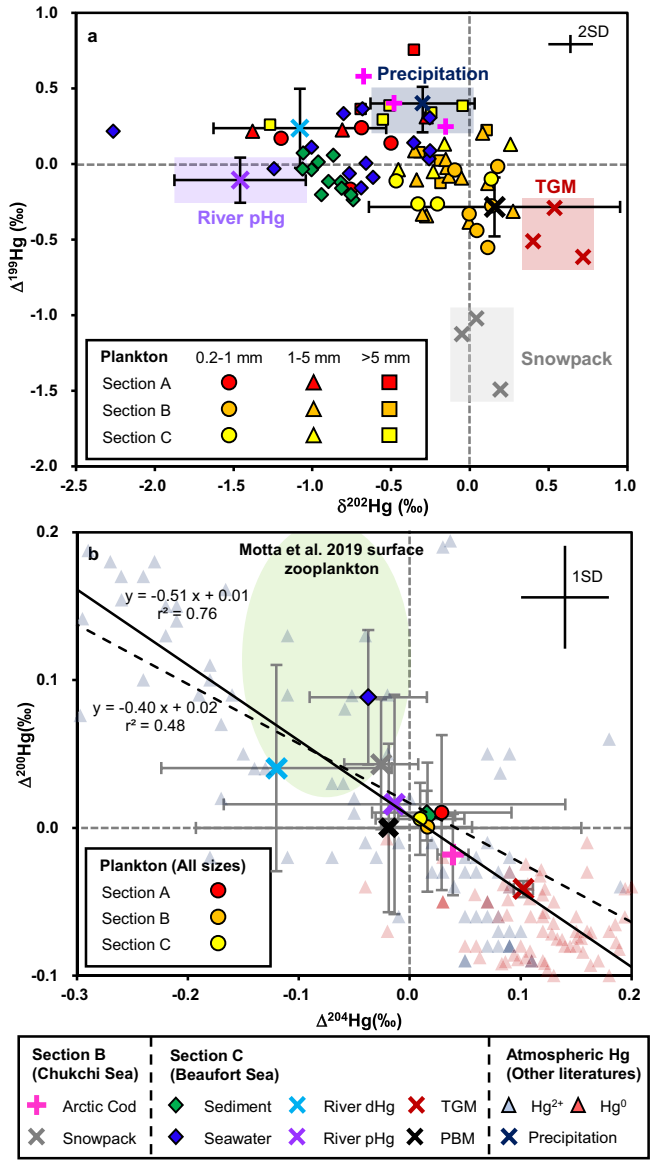

Fig. 2 | Hg isotope values of the Arctic biota and potential endmembers. **a** δ^{202}Hg and Δ^{199}Hg, and b. Δ^{200}Hg and Δ^{204}Hg of zooplankton by section, total gaseous Hg (TGM), snowpack, sediment, and seawater from this study. Hg isotope values of riverine dissolved (River dHg) ($n = 13$, average, 1 SD) and particulate bound Hg (River pHg) ($n = 13$, average, 1 SD) are from the Mackenzie River[38]. Precipitation values are compiled by Jiskra et al.[43], sampled at various regions of the world ($n = 106$, median, quartile), and particulate bound Hg (PBM) values are from Alert, Canada[37] ($n = 10$, average, 1 SD). A green circle indicates Hg isotope ranges of surface zooplankton in the Central Pacific Ocean[65] ($n = 6$, average, 1 SD). Solid line represents Δ^{200}Hg/Δ^{204}Hg slope of atmospheric species (Hg(0), Hg(II); $n = 219$)[32,37,60,61,63–66], and dotted line represents Δ^{200}Hg/Δ^{204}Hg slope of zooplankton (Section A: $n = 9$, Section B: $n = 22$, Section C: $n = 13$), sediment ($n = 11$), seawater ($n = 13$), TGM ($n = 3$), Arctic cod ($n = 3$), snowpack ($n = 3$), PBM, river dHg, and pHg[38] (average, 1 SD, respectively). Analytical errors by reference materials are listed. Source data are provided as a Source Data file.

similar to the trend of MeHg biomagnification in aquatic food webs[29,30,57,58]. With respect to the sampled location, the Section B zooplankton show the highest THg (90.4 ± 31.9 ng g^{-1}, $n = 6$) relative to Section A (25.3 ± 20.4 ng g^{-1}, $n = 4$) and C (57.0 ± 21.9 ng g^{-1}, $n = 4$). In fact, there is a significant positive relationship between zooplankton THg and distances away from land across the studied regions (Supplementary Fig. 3; regression; $p < 0.05$), possibly due to the exposure of spatially different Hg sources.

In regard to Hg isotopes, all zooplankton, regardless of size and location, and the Arctic cods exhibit intermediate δ^{202}Hg and Δ^{199}Hg to that of various environmental matrices (TGM, snowpack, seawater, sediment) characterized in this study and with the global average precipitation[43], atmospheric particulate bound Hg (PBM) from Alert, Canada[37], and dissolved (River dHg) and particulate Hg phases (River pHg) of the Mackenzie River waters[38] (Fig. 2a, Source Data). The relative importance of these environmental matrices acting as potential Hg sources to zooplankton is discussed below. The zooplankton exhibit increasing Δ^{199}Hg with size fractions and % MeHg, but not with δ^{202}Hg (Source Data, Supplementary Fig. 4). The Section B zooplankton, sampled in the open ocean of the Chukchi Sea, have positive δ^{202}Hg and negative Δ^{199}Hg, similar to that of TGM, when compared to the zooplankton at Section A and C (Fig. 2a, Supplementary Fig. 5).

The Δ^{200}Hg and Δ^{204}Hg values (referred to as even-MIF) have been used as indicators to quantify the relative deposition of atmospheric Hg(0) and Hg(II) to the biosphere. This is because measurable Δ^{200}Hg and Δ^{204}Hg changes occur only via Hg(0) photo-oxidation in the troposphere, resulting in a Δ^{200}Hg/Δ^{204}Hg slope of −0.51 ± 0.04[44,59] ($p < 0.05$, $r^2 = 0.76$, $n = 219$; Fig. 2b). This slope has previously been established by the collection and evaluation of Δ^{200}Hg and Δ^{204}Hg data measured from various atmospheric samples[59]. All analyzed samples, atmospheric PBM from Alert, Canada, and the river dHg and pHg from the Mackenzie River[38] depict a slope (−0.40 ± 0.08, $p < 0.05$, $r^2 = 0.48$, $n = 113$), similar to the theoretical Hg(0) photo-oxidation (Fig. 2b). The near-zero Δ^{200}Hg and Δ^{204}Hg of our zooplankton, Arctic cod, sediment, atmospheric PBM, and river pHg[38] are higher than the measured and compiled TGM[32,43,60–64] but lower than zooplankton from the Central Pacific Ocean[65], global precipitation[37,43,60,62,63,65,66], and our seawater, which mostly reflect Hg(II). The snowpack and river dHg[38] have intermediate Δ^{200}Hg values, reflecting mixtures of Hg(0) and Hg(II).

In summary, the near-zero Δ^{200}Hg observed in all zooplankton and the Arctic cods are consistent with Hg(0) but contrast with the positive Δ^{200}Hg of the seawater, reflecting Hg(II). The zooplankton in the open ocean of the Chukchi Sea (Section B) have Hg isotopic compositions particularly similar to that of TGM. Lastly, the % MeHg and Δ^{199}Hg increase with zooplankton sizes to fish, which is a typical pattern of MeHg biomagnification in aquatic food web[29,30]. On the basis of contrasting Δ^{200}Hg values between the biota and seawater, we hypothesize that there may be specific pools of Hg in seawater, which are preferentially bioavailable for zooplankton and fish. Since Hg(0) has to be oxidized to become bioavailable[49–51], we also speculate that Hg(0) has undergone some oxidation processes, which do not impart significant even-MIF, prior to methylation and bioaccumulation in the Arctic Ocean.

Sources and pathways of Hg(0) uptake by zooplankton

While the prevalence of Hg(0) in the Arctic atmosphere is well established, mediated via global transport[4,9,67], snowpack Hg(II) photoreduction[32], and Hg(0) evasion from the ocean surface[4,25,32,68,69], our study documented the widespread Δ^{200}Hg in the Arctic Ocean zooplankton and fish. Here, we apply the global end-member Δ^{200}Hg of Hg(0) (median; −0.05‰, quartiles; −0.08‰, −0.03‰) and Hg(II) (median; 0.14‰, calculated based on precipitation, reactive Hg(II)), estimated by Jiskra et al. 2021[43], to the Eq. (1)-(2) to quantify % contributions of Hg species. The same end-members were used by Jiskra et al. 2021[43] to estimate Hg(0) and Hg(II) deposition to the global seawater. The proportions of Hg(0) and Hg(II) are represented as $f_{Hg(0)}$ and $f_{Hg(II)}$.

$$\Delta^{200}Hg_{sample} = \Delta^{200}Hg(II) \times f_{Hg(II)} + \Delta^{200}Hg(0) \times f_{Hg(0)} \quad (1)$$

$$1 = f_{Hg(II)} + f_{Hg(0)} \quad (2)$$

We estimate that the zooplankton and Arctic cod have, on average, 71 ± 20% (small; 70 ± 20%, medium; 74 ± 21%, large; 67 ± 20%) and 83 ± 15% of Hg originated in the form of Hg(0), respectively (Supplementary Data. 1). The site-specific Hg(0) contribution is difficult to estimate here, given the relatively small Δ^{200}Hg variation in the zooplankton sampled across varying locations.

The high estimated Hg(0) contributions in the Arctic Ocean zooplankton and fish are puzzling since experimental studies have repeatedly demonstrated that Hg(0) uptake by zooplankton is impossible and it would require Hg(0) to be oxidized to modulate passive uptake via the cellular membrane[49–51]. The near-zero Δ^{200}Hg of our biota also contrasts with the positive Δ^{200}Hg of the seawater, reflecting Hg(II) that has undergone oxidation and deposition from the troposphere. Since even-MIF anomalies are generated exclusively in the troposphere under UVC-light and not in aqueous solution[70,71], atmospheric Hg(0) dissolution followed by oxidation in seawater is unlikely to be the primary pathway generating bioavailable Hg(II) in the seawater. Instead, there are already well-established Hg(0) oxidation pathways near the surface in the Arctic[63,72,73], which do not impart even-MIF anomalies and may supply bioavailable Hg(II). The first oxidation pathway is Hg(0) uptake by terrestrial media followed by oxidation within foliar tissues. Especially in the Arctic, it is estimated that Hg(0) uptake by tundra vegetation accounts for 70% of total atmospheric Hg deposition relative to direct Hg(II) input[63,72]. This pathway currently explains the globally observed near-zero Δ^{200}Hg in foliage, litter[72,74] and peat core, used to model historical Hg(0) levels in the Arctic atmosphere[75]. Given the large gross Hg(0) flux to terrestrial ecosystem (118 ± 20 Mg yr^{-1}) followed by riverine discharge to the Arctic Ocean (41 ± 4 Mg yr^{-1})[4,6–8], this may explain the near-zero Δ^{200}Hg in our zooplankton, fish, and river pHg from the Mackenzie River (Fig. 2b). The second pathway is Hg(0) oxidation at the marine boundary layer or near the land surface given the abundances of sea salt aerosols[52,76–78] and bromine radicals liberated from snowpack and sea ice in the Arctic[52,77,79]. Hg(0) oxidation via bromine radicals recorded at a few meters above the snow surface is what drives substantial Hg(II) deposition to the Arctic snowpack during AMDE[76,80,81]. In contrary to the tropospheric oxidation, which imparts positive Δ^{200}Hg in Hg(II) [82,83], this process is thought to leave negative to near-zero Δ^{200}Hg (−0.08 ± 0.04‰; $n = 9$)[32,52,84] in the AMDE-affected snow. Isotopic characterizations of atmospheric samples in Alert, Canada have also found that Hg(0) oxidation followed by particulate Hg(II) scavenging preserves near-zero Δ^{200}Hg in PBM[32,37].

In sum, our proposed Hg sources are no different from the global consensus that Hg in the open ocean waters and biota originates from atmospheric Hg(II) deposition[65,85] and that the Arctic Ocean receives a substantial amount of Hg(II) via riverine export[7,8,17,69]. The difference is the pathway/location at which Hg(0) is oxidized to supply bioavailable Hg(II) in the mid-latitude ocean and the Arctic Ocean biota. In the mid-latitude oceans, Hg(0) oxidation in the troposphere followed by rain and particulate scavenging explain positive Δ^{200}Hg (0.07 ± 0.04‰) observed in both the seawater and biota[19,58,65,85,86]. While this process explains Hg(II) in the Arctic Ocean seawater, Hg(II) that is preferentially available for zooplankton uptake is supplied by Hg(0) oxidation via terrestrial vegetation and at the land/ocean surface, mediated by bromine radicals[52,77,79] and sea salt aerosols[52,76–78]. Apart from the seawater measured in this study and in the Canadian Arctic Archipelago (0.23 ± 0.16‰)[33], oxidation in the troposphere still plays some role in supplying Hg(II) to other abiotic matrices including snow and riverine water (Fig. 2b). Even then, these sources are not as actively utilized by the zooplankton and fish.

Evidence of Hg isotope difference between seawater and biota has previously been documented by Motta et al.[87] in the Central Pacific Ocean. In that study, the authors recorded overlapping δ^{202}Hg between marine particles and MeHg, estimated using the Pacific Ocean fish, to suggest that marine particles act as the main substrate for microbial methylation and bioaccumulation at the base of the food web. The consistent Δ^{200}Hg and Δ^{204}Hg between atmospheric PBM, marine particles, and zooplankton, which differed significantly from the values of precipitation Hg(II) and seawater, further implied that atmospheric PBM supplies marine particles available for methylation in the open ocean. Similarly, at Section C, the δ^{202}Hg, Δ^{199}Hg, and Δ^{200}Hg of the seawater and sediment are within the ranges of dHg and pHg of the Mackenzie River waters, respectively[38] (Fig. 3). Based on the

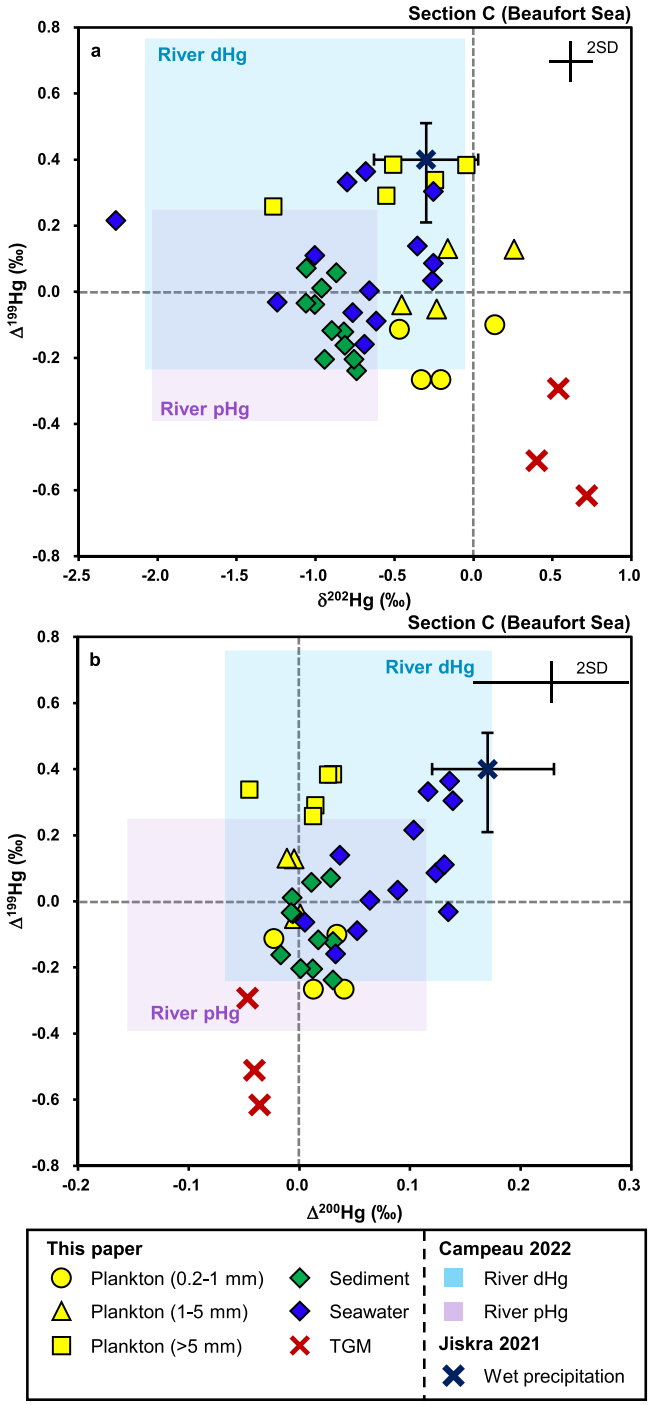

Fig. 3 | Hg isotope ratios of the Beaufort Sea samples. a δ^{202}Hg and Δ^{199}Hg and (**b**) Δ^{200}Hg and Δ^{199}Hg of total gaseous mercury (TGM), sediment, seawater, and zooplankton measured at Section C. Ranges of Hg isotope values of riverine dissolved (River dHg; $n = 13$) and riverine particulate-bound Hg (River pHg; $n = 13$) are from Campeau et al. 2022[38], and the median precipitation is from Jiskra et al. 2021[43] ($n = 106$, median, quartile). Source data are provided as a Source Data file.

overall positive Δ^{200}Hg and the estimated % Hg(II) (63%) relative to Hg(0) in the river dHg, Campeau et al. 2022[38] suggested that river dHg is partly sourced from wet Hg(II) deposition, which has circulated through continental watersheds via throughfall. A portion of river pHg, reflecting Hg(0) sequestered by terrestrial vegetation, is deposited to the sediment during riverine export. The river dHg (originated from wet Hg(II) deposition) acting as a source of the nearshore Beaufort Sea water is further depicted by the relationships between surface seawater profiles and our seawater Δ^{199}Hg and Δ^{200}Hg (Supplementary Fig. 6). The surface seawater Δ^{199}Hg and Δ^{200}Hg reveal significant negative relationships with increasing distances away from the Mackenzie River, salinity, and dissolved oxygen, and significant positive relationships with water temperature and chlorophyll A (all $p < 0.05$). The reduction in Δ^{199}Hg and Δ^{200}Hg toward the near-zero value of Hg(0) suggests that the Arctic Ocean seawater reflects mixtures of Hg(II) exported from the river in dissolved phases and Hg(0) oxidized near the surface. The uniform zooplankton Δ^{200}Hg (Fig. 3b) indicates that they mostly integrate oxidized Hg(0) regardless of the distance away from the Mackenzie River.

As such, the Hg isotope difference between seawater and biota, documented both in the Central Pacific[87] and the Beaufort Sea, would be well explained if bioavailable Hg(II) pools in seawater are in particulate phases. To further describe the overall processes, we propose that Hg(0) oxidized and introduced in the form of atmospheric PBM or riverine pHg act as a substrate for microbial aggregation and methylation in seawater, which further enhances Hg/MeHg bioaccumulation. The Arctic atmosphere is well-known for high proportions of PBM, due to the abundance of sea salt, relative to reactive gaseous Hg(II) (PBM/RGM = 1.42), making atmospheric PBM widely available for deposition to seawater[88]. A recent experimental study has also reported higher methylation rates in unfiltered seawater relative to filtered seawater, suggesting that methylation occurs more actively in the presence of particles[89]. In addition to atmospherically deposited PBM, river pHg has also been reported to serve as a substrate for microbial aggregation and methylation, resulting in up to 85% of MeHg on particles sampled near riverine basins of the Arctic Ocean[90–93].

Thus, we designate atmospheric PBM and river pHg, both of which originated from Hg(0), and precipitation (Hg(II)) as potential Hg sources to the zooplankton and use a ternary mixing model to calculate % source contribution to our zooplankton (Eq. (3)–(5), Supplementary Table. 1). We estimate the isotopic composition of PBM using our TGM and the isotopic difference between PBM and TGM established in Alert, Canada (δ^{202}Hg shift by −0.51‰, Δ^{199}Hg shift by −0.05‰)[37]. Note that kinetic fractionation via oxidation and particle sorption both cause more negative δ^{202}Hg and slightly more negative Δ^{199}Hg in PBM relative to TGM[37,70,94]. While all zooplankton are used for the calculation of % Hg source contribution (Supplementary Data. 1), we report the zooplankton of small size fractions given that they best reflect environmental Hg sources at the base of the food web. We do not consider snowpack as an important Hg source based on the highly negative Δ^{199}Hg (Fig. 2a) and prior modeling studies, which estimated a low Hg influx via snow and ice melting[11,69].

$$\delta^{202}Hg_{sample} = \delta^{202}Hg_a \times f_a + \delta^{202}Hg_b \times f_b + \delta^{202}Hg_c \times f_c \quad (3)$$

$$\Delta^{199}Hg_{sample} = \Delta^{199}Hg_a \times f_a + \Delta^{199}Hg_b \times f_b + \Delta^{199}Hg_c \times f_c \quad (4)$$

$$1 = f_a + f_b + f_c \quad (5)$$

In the open ocean of the Chukchi Sea (Section B), the zooplanktons reflect 72 ± 22% of PBM, 28 ± 22% of precipitation, and 0 ± 0% of river pHg (Kruskal-Wallis test; $p < 0.05$; Supplementary Table. 2). In the Beaufort Sea (Section C), the zooplankton reveal 55 ± 11% contribution of PBM, 30 ± 12% of precipitation, and 14 ± 12% of river pHg (Kruskal-Wallis test; $p < 0.05$). The zooplankton near the Bering Strait (Section A) show stronger river pHg contribution (42 ± 18%) and precipitation (46 ± 23%), followed by PBM (13 ± 16%), in line with the larger estimated annual Hg export from the Yukon River (3282 kg y^{-1}) relative to the Mackenzie River (2610 kg y^{-1})[8] (Kruskal-Wallis test; $p = 0.08$).

Implications to the Arctic Ocean food web

A compilation of Δ^{200}Hg in the Arctic Ocean biota, particularly those located at high trophic positions (ringed seal, polar bear, beluga whale, murre egg), display uniform near-zero values (0.01 ± 0.03‰, $n = 128$; 1 SD)[34,41,42] (Supplementary Fig. 7). Even freshwater fish surveyed across the Arctic lake systems have suppressed Δ^{200}Hg (0.05 ± 0.05‰; n = 65)[39] relative to fish from the Great Lakes, U.S (0.07 ± 0.03‰; $n = 135$)[95], which mostly receive wet deposited Hg(II). While the even-MIF anomalies reveal the pathways of Hg(0) oxidation and incorporation into biota, other Hg isotope signatures (MDF, odd-MIF) also provide insights into the pathways of MeHg formation and degradation within the water column. From the perspective of Hg isotopic pattern, we further summarize sources and processes, leading to MeHg bioaccumulation across several studied marine food webs.

In the Central Pacific Ocean, Blum et al. 2013[19] suggested that atmospherically deposited Hg(II) acts as a single dominant source, which is primarily methylated at the oxygen minimum zone, circulated to the mixed layer and deeper depth via sinking, and photo-degraded at varying extents. This leaves zooplankton and fish with a Δ^{199}Hg/δ^{202}Hg slope (2.32 ± 0.23; $p < 0.05$, $r^2 = 0.82$, $n = 86$)[19,65] consistent with experimentally derived MeHg photo-degradation in aqueous solution (2.43 ± 0.10)[96] (Fig. 4a). The positive Δ^{200}Hg in the zooplankton and fish at the Pacific Ocean as well as the consistent Δ^{200}Hg between the zooplankton and marine particles, originated from atmospheric PBM, now suggest that Hg(0) oxidized in the troposphere, scavenged by particles, and methylated in the water column is the main source to the mid-latitude ocean food web.

A similar isotopic pattern is revealed in the Bering Strait food web (Section A), except for the substantially depressed Δ^{199}Hg/δ^{202}Hg slope (0.18 ± 0.05, $p < 0.05$, $r^2 = 0.62$, $n = 27$). The Bering Strait food web shown in Fig. 4b encompasses the Section A zooplankton and the estimated isotopic compositions of prey (mostly cod) consumed by ringed seal and polar bear sampled at Norton Sound[34] (red box; Fig. 1) (Supplementary Information). As estimated in this study, river pHg (Hg(0) oxidation via foliar tissue) is an important Hg source to the Section A zooplankton and supplies the site for microbial methylation and photo-degradation prior to ecological exposure. In addition to photo-degradation, the depressed Δ^{199}Hg/δ^{202}Hg slope indicates that there is active microbial demethylation, which typically enriches δ^{202}Hg of the remaining MeHg[97,98]. Similarly depressed slopes have been recorded in the food webs of the Bohai Sea[57], Gulf of Mexico[58], and across the northeast estuaries in the U.S[29]., all influenced by riverine Hg sources. Terrestrial organic matter exported from the Arctic rivers is thought to promote the growth of microbial communities and primary productivity[93], which may, in turn, enhance the extent of biotic demethylation and Hg biodilution[90]. This would also explain the low THg observed in the Section A zooplankton relative to other locations.

The unusual negative Δ^{199}Hg/δ^{202}Hg slope is observed in the open ocean of the Chukchi Sea food web (Fig. 4c), spanning our Section B zooplankton and Arctic cod, and the estimated isotopic compositions of fish consumed by beluga whales collected offshore of Utqiagvik, Alaska[34] (orange box; Fig. 1) (Supplementary Information). We explain this isotopic pattern by Hg(0) oxidation and deposition in the form of PBM followed by rapid Hg(II) photo-reduction and uptake by surface-dwelling zooplankton. This is evident by the high THg concentration and a Δ^{199}Hg/Δ^{201}Hg slope (0.91 ± 0.12; $p < 0.05$, $r^2 = 0.73$, $n = 22$),

https://doi.org/10.1038/s41467-024-51852-2

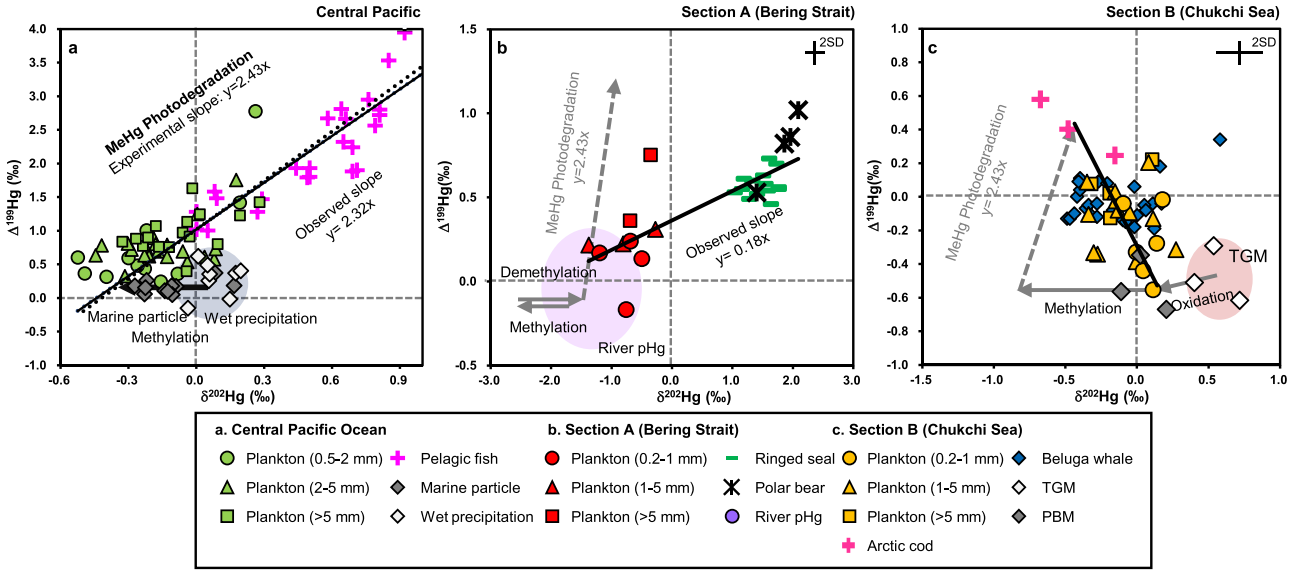

Fig. 4 | Trends of δ^{202}Hg and Δ^{199}Hg in marine biota across different latitudes. **a** Zooplankton and fish from the Central Pacific Ocean[19,65] ($n = 86$), (**b**) Zooplankton from Section A (Bering Strait), ringed seal, and polar bear from Norton Sound[34] ($n = 27$), **c** Zooplankton and Arctic cod from Section B (Chukchi Sea), and the estimated prey item consumed by beluga whales are from the offshore of Utqiagvik, Alaska[34] ($n = 28$). Particulate-bound Hg (PBM) is derived from the measured total gaseous Hg (TGM). Wet precipitation ($n = 8$) and riverine particulate-bound Hg (river pHg; $n = 13$) are from Motta et al. 2019[65] and Campeau et al. 2022[38], respectively. Source data are provided as a Source Data file.

consistent with the experimental Hg(II) photo-reduction, of our Section B zooplankton. The Arctic Ocean has one of the highest THg content in the surface water column relative to deeper depths[21], which may induce active plankton Hg(II) uptake near the surface. A portion of PBM is methylated and photo-degraded during sinking to impart negative δ^{202}Hg and suppressed Δ^{199}Hg in MeHg bioaccumulated into the Arctic cod and other fish utilizing deeper depths (>900 m)[87,99]. In polar marine waters, methylation takes place at both the chlorophyll maximum[26,35] and in the oxycline[25,26], contrasting the mid-latitude oceans where methylation occurs primarily at the oxygen minimum zone[18,19]. The unusually strong stratification in the Arctic Ocean could hinder the circulation of methylated Hg to the mixed layer for further photo-degradation[22,100]. The estimated MeHg δ^{202}Hg prior to photo-degradation, using the average Arctic cod δ^{202}Hg and Δ^{199}Hg and the experimental MeHg photo-degradation slope (DOC; 1 mg L^{-1})[96], reveal a value of −0.83‰. The δ^{202}Hg difference between the estimated MeHg and atmospheric PBM, reflecting Hg(II) (0.86‰), in the Chukchi Sea is measurably higher compared to the Central Pacific Ocean (0.5‰ between marine particles and their estimated MeHg using fish), but similar to the experimental δ^{202}Hg difference during near complete methylation (<0.9‰)[101]. The substantial microbial methylation and suppressed photo-degradation evaluated using the Hg isotope pattern are in strong agreement with the measured data from the Arctic Ocean[21,26,35].

Apart from the Hg isotopic pattern, a vast number of studies from the Arctic Ocean have reported active formation and evasion of dimethylmercury (DMHg) from seawater[11,26,102], which may serve as another important MeHg source to aquatic and terrestrial food webs. The photo-decomposition of DMHg into MeHg and its subsequent deposition back into the environment is estimated to be as high as 8 Mg/yr[11,103], leading to secondary MeHg exposure to terrestrial vegetation (lichen) in coastal landscapes[104]. While the absence of isotopic data on DMHg is primarily attributed to its low concentration, future isotopic characterization would enable a comprehensive understanding of the Arctic Ocean Hg cycle. Isotopic characterization of MeHg in biota would also enhance understanding of processes driving MeHg production and bioaccumulation in the Arctic Ocean food web[105].

It is surprising that much of the Hg(0) oxidized in the troposphere supplies the bioavailable Hg(II) to the mid-latitude oceans since the troposphere occurs at a higher atmospheric column compared to the Arctic. While this still explains the previously documented latitudinal Δ^{200}Hg increase in precipitation sampled across various regions of the world[44] and positive Δ^{200}Hg anomalies in the Arctic seawater[33], the prevalence of near-surface Hg(0) oxidation, caused by coastal halogen and sea salt aerosols, seems to drive rapid Hg(II) input and bioavailable pools to the surface-dwelling zooplankton in the Arctic Ocean. We speculate that this is exacerbated by microbial methylation on particles, which occurs at varying water depths, and suppressed photo-degradation, leading to Hg exposure to the Arctic Ocean food web. Hg(0) oxidation by terrestrial media followed by riverine export is also a relevant source since the Arctic Ocean is completely surrounded by land and receives larger riverine Hg export than other ocean basins. Given the importance of particulate phases acting as the site for microbial methylation and bioaccumulation, assessing the extent of Hg bioaccumulation during AMDEs and spring freshet would allow the understanding of ecological Hg exposures during seasonally unique periods in the Arctic. The contrasting Δ^{199}Hg/δ^{202}Hg pattern between the Arctic Ocean and mid-latitude ocean also merits the future need to study unique Hg oxidation and biogeochemical pathways leading to Hg(II) bioavailability.

Methods

Site description

All samples were collected in the Arctic Ocean on board of the R/V ARAON, operated by the Korea Polar Research Institute (KOPRI). Sampling durations are divided into two cruise campaigns of ARA13B (July 21st to August 20th, 2022) and ARA13C (August 26th to September 12th, 2022) (Fig. 1a, b). As illustrated in Fig. 1a, ARA13B is divided into two geographic sections of the Bering Strait and the Chukchi Sea (Section A, B). ARA13C is characterized as the Beaufort Sea and the Mackenzie River estuaries, located 650-850 km away from Utqiagvik (Section C; Fig. 1b). All sampling procedures were approved by Alaska Fisheries Science Center, National Oceanic and Atmospheric Administration, USA (U2022-005) for Section A and B. All sampling procedures conducted in Section C were approved by the Inuvialuit

Environmental Impact Screening Committee (EISC Registry File: 01-22-08), the Government of Northwest Territories (License No. 16995), the Government of Yukon (License No. 22-11S&E) and Trade and Development Canada (Permit-IGR-1283).

Sample collection

During ARA13C (Section C; Fig. 1b), atmospheric samples of total gaseous mercury (TGM) and precipitation were sampled during the entire cruise campaign and at the compass deck to avoid vessel emissions. Samples of surface sediment, seawater, and zooplankton were collected at varying depths and at locations away from the Mackenzie River (Source Data, Supplementary Data 2). TGM was collected onto a gold trap (Brooksrand instruments) by pumping air through a PTFE syringe filter (pore size: 0.45 um, ϕ: 25 mm) and soda trap (Sigma Aldrich) at a flow rate of 1.94 L min^{-1}. Rain event occurred once on the 25th of August, which was sampled for two hours in a 1 L FEP bottle pre-treated with 10 mL of 50% HCl. Each bottle was connected to an acid-washed 136 mm diameter Pyrex funnel and a p-trap. Precipitation was then preserved at 4°C prior to analyses.

Sediment was collected at the surface (0 to 3 cm depth) and at 11 sites (C.01-C.11; Fig. 1b) using a multi-corer (MUC 8 multi-corer, Oktopus GmbH, Germany), equipped with eight polycarbonate coring tubes (length: 80 cm, ϕ: 10.5 cm). Samples were placed in an acid-washed 50 mL polypropylene conical tube and stored at −70°C. Seawater was collected at the surface and the subsurface Chlorophyll Maxima (SCM) at five sites (C.01-C.04, C.07) using a CTD/rosette, equipped with acid-cleaned 10 L Niskin bottles with SBE9plus CTD profiler. Each site and depth were profiled with temperature, dissolved oxygen, salinity, and fluorescence (Supplementary Table 3). Seawater was transferred into a 20 L polycarbonate bottle or a 10 L Pyrex glass bottle, precleaned with 40% HNO_3 and 10% HCl and equipped with a Teflon cap. All samples were kept in the dark after being treated with 5% BrCl. Zooplankton were collected at the surface and the SCM from 2 sites (C.02, C.04; Fig. 1b) using a Bongo plankton net (mesh size: 150 um). At each sampling location and depth, seawater properties were measured using a CTD. The bongo net was operated at a speed of 40 m min^{-1} upward, 60 m min^{-1} downward and maintained for 20 seconds at targeted depths. Each sampling was conducted with a flowmeter mounted in the mouth of a bongo net to calculate the abundance of zooplankton. Sampled zooplankton were sieved into three size fractions of 0.2–1 mm, 1–5 mm, and >5 mm with an acid-washed filtering device (47 mm diameter, 0.2 mm synthetic nylon mesh filters) and preserved at −70 °C in petri dish.

During ARA13B (Section A, B; Fig. 1a, Supplementary Fig. 1), snowpack, zooplankton, and fish samples were collected at varying locations. Zooplankton were collected using the same method as Section C at varying depths including the surface (Source Data, Supplementary Data.2). Three individuals of Arctic cod were sampled regardless of gender at Section B (Beaufort Sea) to evaluate the extent of Hg bioaccumulation. All fish were euthanized using 95% ethanol and preserved at −25 °C following the protocol[106]. Surface snowpack (0 to 1 cm) was collected on an Arctic Ocean ice sheet (Supplementary Fig. 1), using an acid-washed Teflon scoop. Samples were placed in a 2.2 L FEP bottle, cleaned with acetone, Citranox soap, 10% HNO_3, and BrCl (Douglas and Blum 2019[107]), and stored at −25 °C.

Hg and MeHg concentration analyses

All samples were transported to the Environmental Health and Assessment Laboratory, Pohang University of Science and Technology (POSTECH) on the cruise. For solid samples of zooplankton, fish, and sediment, the samples were lyophilized, homogenized, and measured for total Hg (THg) concentration using a Nippon Instruments MA-3000 Hg analyzer. NRC-TORT-3 (lobster) and NIST-2711A (Montana soil) were used to verify the accuracy of the analysis, which resulted in THg recoveries of 97.4 ± 6.4% (n = 5, 1 SD) and 94.1 ± 0.3% (n = 2). MeHg concentration was measured for zooplankton by digesting the lyophilized sample in 30% HNO_3 for 12 h at 75 °C and measuring them using a CVAFS connected with a gas chromatography (GC). NRC-TORT-3 was digested in the same way to verify the procedure, which has MeHg recovery of 93.0% ± 0.1% (n = 2, 1 SD).

TGM sampled onto the gold traps were heated, purged, and trapped into 1% $KMnO_4$ in 10% H_2SO_4 (wt/wt) via Hg-free air. Snow was thawed at room temperature in the dark and digested with 10% HCl and 1% BrCl for 1 month. Precipitation, which had a total mass of 91.5 g, and seawater were treated with HCl and BrCl to achieve 2% and 4% by volume, respectively, and measured for THg using a cold vapor atomic fluorescence spectrophotometry (CVAFS; Brooksrand instruments, 99.4 ± 4.1%; n = 11, 1 SD).

Hg isotope analyses

Solid samples of zooplankton, fish, and surface sediment were loaded onto a dual-stage thermal combustion furnace to release all Hg in the form of Hg(0). The released Hg was transferred into a 1% $KMnO_4$ in a 10% H_2SO_4 (wt/wt) solution. Seawater sampled at each site and depth was allocated into four 10 L Pyrex bottles and preconcentrated into a 6 mL 40% reverse aqua regia (HNO_3/HCl=2:1 (v/v)), following the method by Jiskra et al. 2021[43]. To describe the procedure, each seawater bottle was purged with high purity argon gas using a bubbler glass post (P3 porosity frit) for 16 h at 300 mL min^{-1}. During purging, 10% $NH_2OH \cdot HCl$ was added to neutralize excess BrCl and 100 mL of $SnCl_2$ was added to reduce all Hg(II) to Hg(0). Trapped solutions were preconcentrated into a 6 mL (volume) of 40% reverse aqua regia by purging with high purity argon gas for 3 h. Snow samples (1 L) were treated the same way and trapped into a 40% reverse aqua regia.

All samples in either 1% $KMnO_4$ solutions or 40% reverse aqua regia were neutralized with 30% $NH_2OH \cdot HCl$. 40% reverse aqua regia solutions were then diluted to 20% reverse aqua regia. Each sample was measured for THg concentration using a CVAFS to calculate the THg recoveries from combustion and preconcentration steps. The average THg recovery of zooplankton, fish, and sediment was 103.8 ± 19.9% (n = 17, 1 SD) for the available samples and the snow had an average THg recovery of 111.8 ± 7.4% (n = 3). NRC-TORT-3 (lobster) and NIST-2711A (Montana soil) for solid samples had THg transfer recoveries of 99.6 ± 8.0% (n = 7, 1 SD) and 89.9 ± 2.0% (n = 4, 1 SD). The THg recoveries for the seawater preconcentration steps were estimated by spiking 12 ng of Hg from NIST SRM 8610 into 20 L distilled water. The preconcentration steps yielded an average THg recovery of 88.5 ± 5.5% (n = 4, 1 SD).

Hg stable isotopes were measured using a multi-collector inductively coupled plasma mass spectrometer (MC-ICP-MS; Nu instruments) with a reducing agent of 2% $SnCl_2$ connected to a gas-liquid separator. Instrumental mass bias was corrected using an internal Thallium standard (NIST SRM 997) introduced with a nebulizer and NIST SRM 3133 was used to bracket each sample with the same matrix and THg concentrations. MDF is reported as δ^{202}Hg (‰) referenced to NIST SRM 3133 and MIF is reported as Δ^{199}Hg, Δ^{200}Hg, Δ^{201}Hg, Δ^{204}Hg (‰)[108] (Supplementary Information, Supplementary Table. 4).

Reporting summary

Further information on research design is available in the Nature Portfolio Reporting Summary linked to this article.

Data availability

Bathymetric data was extracted from the GEBCO_2022 Grid, GEBCO Compilation Group (2022) GEBCO 2022 Grid [https://doi.org/10.5285/e0f0bb80-ab44-2739-e053-6c86abc0289c] for Fig. 1 and Supplementary Fig. 1. All data generated in this study are provided in the Source Data file and are available under accession code [https://doi.org/10.6084/m9.figshare.24995960]. Detailed information regarding the calculation of % Hg source contribution and zooplankton sampling information (time, location) are shown in Supplementary Data 1 and 2,

respectively. Additional information is shown in the Supplementary Information file, which are all available for download from Nature Communications. Source data are provided with this paper.

References

1. Krabbenhoft, D. P. & Sunderland, E. M. Global change and mercury. *Science* **341**, 1457–1458 (2013).
2. Driscoll, C. T., Mason, R. P., Chan, H. M., Jacob, D. J. & Pirrone, N. Mercury as a global pollutant: sources, pathways, and effects. *Environ. Sci. Technol.* **47**, 4967–4983 (2013).
3. Streets, D. G. et al. Global and regional trends in mercury emissions and concentrations, 2010–2015. *Atmos. Environ.* **201**, 417–427 (2019).
4. Dastoor, A. et al. Arctic mercury cycling. *Nat. Rev. Earth Environ.* **3**, 270–286 (2022).
5. Petrova, M. V. et al. Mercury species export from the Arctic to the Atlantic Ocean. *Mar. Chem.* **225**, 103855 (2020).
6. Durnford, D. et al. How relevant is the deposition of mercury onto snowpacks? – Part 2: A modeling study. *Atmos. Chem. Phys.* **12**, 9251–9274 (2012).
7. Sonke, J. E. et al. Eurasian river spring flood observations support net Arctic Ocean mercury export to the atmosphere and Atlantic Ocean. *Proc. Natl. Acad. Sci. USA.* **115**, E11586–E11594 (2018).
8. Zolkos, S. et al. Mercury export from arctic great rivers. *Environ. Sci. Technol.* **54**, 4140–4148 (2020).
9. Schartup, A. T., Soerensen, A. L., Angot, H., Bowman, K. & Selin, N. E. What are the likely changes in mercury concentration in the Arctic atmosphere and ocean under future emissions scenarios? *Sci. Total Environ.* **836**, 155477 (2022).
10. Fisher, J. A. et al. Factors driving mercury variability in the Arctic atmosphere and ocean over the past 30 years. *Glob. Biogeochem. Cycles* **27**, 1226–1235 (2013).
11. Soerensen, A. L. et al. A mass budget for mercury and methylmercury in the Arctic Ocean: ARCTIC OCEAN HG AND MEHG MASS BUDGET. *Glob. Biogeochem. Cycles* **30**, 560–575 (2016).
12. Kumar, A. & Wu, S. Mercury pollution in the arctic from wildfires: Source attribution for the 2000s. *Environ. Sci. Technol.* **53**, 11269–11275 (2019).
13. Dietz, R. et al. A risk assessment review of mercury exposure in Arctic marine and terrestrial mammals. *Sci. Total Environ.* **829**, 154445 (2022).
14. Barst, B. D., Chételat, J. & Basu, N. Toxicological risk of mercury for fish and invertebrate prey in the Arctic. *Sci. Total Environ.* **836**, 155702 (2022).
15. Mason, R. P. et al. Mercury biogeochemical cycling in the ocean and policy implications. *Environ. Res.* **119**, 101–117 (2012).
16. Fitzgerald, W. F., Lamborg, C. H. & Hammerschmidt, C. R. Marine biogeochemical cycling of mercury. *Chem. Rev.* **107**, 641–662 (2007).
17. Liu, M. et al. Rivers as the largest source of mercury to coastal oceans worldwide. *Nat. Geosci.* **14**, 672–677 (2021).
18. Sunderland, E. M., Krabbenhoft, D. P., Moreau, J. W., Strode, S. A. & Landing, W. M. Mercury sources, distribution, and bioavailability in the North Pacific Ocean: Insights from data and models. *Glob. Biogeochem. Cycles* **23**, 2008GB003425 (2009).
19. Blum, J. D., Popp, B. N., Drazen, J. C., Anela Choy, C. & Johnson, M. W. Methylmercury production below the mixed layer in the North Pacific Ocean. *Nat. Geosci.* **6**, 879–884 (2013).
20. Mazrui, N. M., Jonsson, S., Thota, S., Zhao, J. & Mason, R. P. Enhanced availability of mercury bound to dissolved organic matter for methylation in marine sediments. *Geochimica et. Cosmochimica Acta* **194**, 153–162 (2016).
21. Bowman, K. L., Lamborg, C. H. & Agather, A. M. A global perspective on mercury cycling in the ocean. *Sci. Total Environ.* **710**, 136166 (2020).
22. Heimbürger, L.-E. et al. Shallow methylmercury production in the marginal sea ice zone of the central Arctic Ocean. *Sci. Rep.* **5**, 10318 (2015).
23. Wang, K. et al. Subsurface seawater methylmercury maximum explains biotic mercury concentrations in the Canadian Arctic. *Sci. Rep.* **8**, 14465 (2018).
24. Schartup, A. T. et al. Freshwater discharges drive high levels of methylmercury in Arctic marine biota. *Proc. Natl Acad. Sci. Usa.* **112**, 11789–11794 (2015).
25. Kirk, J. L. et al. Methylated mercury species in marine waters of the canadian high and sub arctic. *Environ. Sci. Technol.* **42**, 8367–8373 (2008).
26. Lehnherr, I., St. Louis, V. L., Hintelmann, H. & Kirk, J. L. Methylation of inorganic mercury in polar marine waters. *Nat. Geosci.* **4**, 298–302 (2011).
27. Schroeder, W. H., Anlauf, K. G., Barrie, L. A., Lu, J. Y. & Steffen, A. Arctic springtime depletion of mercury. *Nature* **394**, 331–332 (1998).
28. Basu, N. et al. The impact of mercury contamination on human health in the Arctic: A state of the science review. *Sci. Total Environ.* **831**, 154793 (2022).
29. Kwon, S. Y., Blum, J. D., Chen, C. Y., Meattey, D. E. & Mason, R. P. Mercury isotope study of sources and exposure pathways of methylmercury in estuarine food webs in the Northeastern U.S. *Environ. Sci. Technol.* **48**, 10089–10097 (2014).
30. Kwon, S. Y., Blum, J. D., Nadelhoffer, K. J., Timothy Dvonch, J. & Tsui, M. T.-K. Isotopic study of mercury sources and transfer between a freshwater lake and adjacent forest food web. *Sci. Total Environ.* **532**, 220–229 (2015).
31. Li, M.-L. et al. Internal Dynamics and Metabolism of Mercury in Biota: A Review of Insights from Mercury Stable Isotopes. *Environ. Sci. Technol.* **56**, 9182–9195 (2022).
32. Araujo, B. F. et al. Mercury isotope evidence for Arctic summertime re-emission of mercury from the cryosphere. *Nat. Commun.* **13**, 4956 (2022).
33. Štrok, M., Baya, P. A. & Hintelmann H. The mercury isotope composition of Arctic coastal seawater. *Comptes Rendus Geosci.* **347**, 368–376 (2015).
34. Masbou, J. et al. Hg-stable isotope variations in marine top predators of the western arctic ocean. *ACS Earth Space Chem.* **2**, 479–490 (2018).
35. Agather, A. M., Bowman, K. L., Lamborg, C. H. & Hammerschmidt, C. R. Distribution of mercury species in the Western Arctic Ocean (U.S. GEOTRACES GN01). *Mar. Chem.* **216**, 103686 (2019).
36. Jiskra, M., Sonke, J. E., Agnan, Y., Helmig, D. & Obrist, D. Insights from mercury stable isotopes on terrestrial–atmosphere exchange of Hg(0) in the Arctic tundra. *Biogeosciences* **16**, 4051–4064 (2019).
37. Zheng, W. et al. Mercury stable isotopes reveal the sources and transformations of atmospheric Hg in the high Arctic. *Appl. Geochem.* **131**, 105002 (2021).
38. Campeau, A. et al. Sources of riverine mercury across the Mackenzie River Basin; inferences from a combined Hg C isotopes and optical properties approach. *Sci. Total Environ.* **806**, 150808 (2022).
39. Gantner, N., Hintelmann, H., Zheng, W. & Muir, D. C. Variations in stable isotope fractionation of hg in food webs of arctic lakes. *Environ. Sci. Technol.* **43**, 9148–9154 (2009).
40. DiMento, B. P., Mason, R. P., Brooks, S. & Moore, C. The impact of sea ice on the air-sea exchange of mercury in the Arctic Ocean. *Deep Sea Res. Part I: Oceanographic Res. Pap.* **144**, 28–38 (2019).
41. Day, R. D. et al. Mercury stable isotopes in seabird eggs reflect a gradient from terrestrial geogenic to oceanic mercury reservoirs. *Environ. Sci. Technol.* **46**, 5327–5335 (2012).
42. Point, D. et al. Methylmercury photodegradation influenced by sea-ice cover in Arctic marine ecosystems. *Nat. Geosci.* **4**, 188–194 (2011).

43. Jiskra, M. et al. Mercury stable isotopes constrain atmospheric sources to the ocean. *Nature* **597**, 678–682 (2021).
44. Cai, H. & Chen, J. Mass-independent fractionation of even mercury isotopes. *Sci. Bull.* **61**, 116–124 (2016).
45. Mason, R. P. & Fitzgerald, W. F. The distribution and biogeochemical cycling of mercury in the equatorial Pacific Ocean. *Deep Sea Res. Part I: Oceanogr. Res. Pap.* **40**, 1897–1924 (1993).
46. Mason, R. P., Fitzgerald, W. F. & Morel, F. M. M. The biogeochemical cycling of elemental mercury: Anthropogenic influences. *Geochimica et. Cosmochimica Acta* **58**, 3191–3198 (1994).
47. Kim, J. P. & Fitzgerald, W. F. Sea-air partitioning of mercury in the equatorial pacific ocean. *Science* **231**, 1131–1133 (1986).
48. Poulain, A. J. et al. Biological and chemical redox transformations of mercury in fresh and salt waters of the high arctic during spring and summer. *Environ. Sci. Technol.* **41**, 1883–1888 (2007).
49. Le Faucheur, S., Campbell, P. G. C., Fortin, C. & Slaveykova V. I. Interactions between mercury and phytoplankton: Speciation, bioavailability, and internal handling: Mercury-phytoplankton interactions. *Environ. Toxicol. Chem.* **33**, 1211–1224 (2014).
50. Mason, R. P., Reinfelder, J. R., Morel, F. M. M. & Uptake Toxicity, and trophic transfer of mercury in a coastal diatom. *Environ. Sci. Technol.* **30**, 1835–1845 (1996).
51. Mason, R. P., Morel, F. M. M. & Hemond, H. F. The role of microorganisms in elemental mercury formation in natural waters. *Water, Air, Soil Pollut.* **80**, 775–787 (1995).
52. Sherman, L. S., Blum, J. D., Douglas, T. A. & Steffen, A. Frost flowers growing in the Arctic ocean-atmosphere-sea ice-snow interface: 2. Mercury exchange between the atmosphere, snow, and frost flowers: MERCURY CYCLING AND FROST FLOWERS. *J. Geophys. Res.* **117**, D00R10 (2012).
53. Atwell, L., Hobson, K. A. & Welch, H. E. Biomagnification and bioaccumulation of mercury in an arctic marine food web: insights from stable nitrogen isotope analysis. **55**, (1998).
54. Stern, G. A. & Macdonald, R. W. Biogeographic Provinces of Total and Methyl Mercury in Zooplankton and Fish from the Beaufort and Chukchi Seas: Results from the SHEBA Drift. *Environ. Sci. Technol.* **39**, 4707–4713 (2005).
55. Fox, A. L. et al. Mercury in the northeastern Chukchi Sea: Distribution patterns in seawater and sediments and biomagnification in the benthic food web. *Deep Sea Res. Part II: Topical Stud. Oceanogr.* **102**, 56–67 (2014).
56. Pomerleau, C. et al. Pan-Arctic concentrations of mercury and stable isotope ratios of carbon (δ13C) and nitrogen (δ15N) in marine zooplankton. *Sci. Total Environ.* **551**, 92–100 (2016).
57. Meng, M. et al. Mercury isotope variations within the marine food web of Chinese Bohai Sea: Implications for mercury sources and biogeochemical cycling. *J. Hazard. Mater.* **384**, 121379 (2020).
58. Senn, D. B. et al. Stable Isotope (N, C, Hg) study of methylmercury sources and trophic transfer in the northern Gulf of Mexico. *Environ. Sci. Technol.* **44**, 1630–1637 (2010).
59. Blum, J. D. & Johnson, M. W. Recent developments in mercury stable isotope analysis. *Rev. Mineral. Geochem.* **82**, 733–757 (2017).
60. Demers, J. D., Blum, J. D. & Zak, D. R. Mercury isotopes in a forested ecosystem: Implications for air-surface exchange dynamics and the global mercury cycle: MERCURY ISOTOPES IN A FORESTED ECOSYSTEM. *Glob. Biogeochem. Cycles* **27**, 222–238 (2013).
61. Fu, X. et al. Domestic and transboundary sources of atmospheric particulate bound mercury in remote areas of China: Evidence from mercury isotopes. *Environ. Sci. Technol.* **53**, 1947–1957 (2019).
62. Enrico, M. et al. Atmospheric mercury transfer to peat bogs dominated by gaseous elemental mercury dry deposition. *Environ. Sci. Technol.* **50**, 2405–2412 (2016).
63. Obrist, D. et al. Tundra uptake of atmospheric elemental mercury drives Arctic mercury pollution. *Nature* **547**, 201–204 (2017).
64. Demers, J. D., Sherman, L. S., Blum, J. D., Marsik, F. J. & Dvonch, J. T. Coupling atmospheric mercury isotope ratios and meteorology to identify sources of mercury impacting a coastal urban-industrial region near Pensacola, Florida, USA. *Glob. Biogeochem. Cycles* **29**, 1689–1705 (2015).
65. Motta, L. C. et al. Mercury cycling in the north pacific subtropical gyre as revealed by mercury stable isotope ratios. *Glob. Biogeochem. Cycles* **33**, 777–794 (2019).
66. Kurz, A. Y., Blum, J. D., Johnson, M. W., Nadelhoffer, K. & Zak, D. R. Isotopic composition of mercury deposited via snow into mid-latitude ecosystems. *Sci. Total Environ.* **784**, 147252 (2021).
67. Dastoor, A. et al. Arctic atmospheric mercury: Sources and changes. *Sci. Total Environ.* **839**, 156213 (2022).
68. Chételat, J. et al. Climate change and mercury in the Arctic: Abiotic interactions. *Sci. Total Environ.* **824**, 153715 (2022).
69. Fisher, J. A. et al. Riverine source of Arctic Ocean mercury inferred from atmospheric observations. *Nat. Geosci.* **5**, 499–504 (2012).
70. Sun, G. et al. Mass-dependent and -independent fractionation of mercury isotope during gas-phase oxidation of elemental mercury vapor by atomic Cl and Br. *Environ. Sci. Technol.* **50**, 9232–9241 (2016).
71. Sun, G. et al. Dissociation of mercuric oxides drives anomalous isotope fractionation during net photo-oxidation of mercury vapor in air. *Environ. Sci. Technol.* **56**, 13428–13438 (2022).
72. Zhou, J., Obrist, D., Dastoor, A., Jiskra, M. & Ryjkov, A. Vegetation uptake of mercury and impacts on global cycling. *Nat. Rev. Earth Environ.* **2**, 269–284 (2021).
73. Lindberg, S. E. et al. Dynamic oxidation of gaseous mercury in the arctic troposphere at polar sunrise. *Environ. Sci. Technol.* **36**, 1245–1256 (2002).
74. Wang, X., Yuan, W., Lin, C.-J. & Feng, X. Mercury cycling and isotopic fractionation in global forests. *Crit. Rev. Environ. Sci. Technol.* **52**, 3763–3786 (2022).
75. Enrico, M. et al. Holocene atmospheric mercury levels reconstructed from peat bog mercury stable isotopes. *Environ. Sci. Technol.* **51**, 5899–5906 (2017).
76. Custard, K. D., Raso, A. R. W., Shepson, P. B., Staebler, R. M. & Pratt, K. A. Production and release of molecular bromine and chlorine from the arctic coastal snowpack. *ACS Earth Space Chem.* **1**, 142–151 (2017).
77. Pratt, K. A. et al. Photochemical production of molecular bromine in Arctic surface snowpacks. *Nat. Geosci.* **6**, 351–356 (2013).
78. Abbatt, J. P. D. et al. Halogen activation via interactions with environmental ice and snow in the polar lower troposphere and other regions. *Atmos. Chem. Phys.* **12**, 6237–6271 (2012).
79. Toyota, K., McConnell, J. C., Staebler, R. M. & Dastoor, A. P. Air–snowpack exchange of bromine, ozone and mercury in the springtime Arctic simulated by the 1-D model PHANTAS – Part 1: In-snow bromine activation and its impact on ozone. *Atmos. Chem. Phys.* **14**, 4101–4133 (2014).
80. Douglas, T. A. et al. Frost flowers growing in the Arctic ocean-atmosphere-sea ice-snow interface: 1. Chemical composition: CHEMICAL COMPOSITION OF FROST FLOWERS. *J. Geophys. Res.* **117**, D00R09 (2012).
81. Steffen, A., Schroeder, W., Bottenheim, J., Narayan, J. & Fuentes, J. D. Atmospheric mercury concentrations: measurements and profiles near snow and ice surfaces in the Canadian Arctic during Alert 2000. *Atmos. Environ.* **36**, 2653–2661 (2002).
82. Chen, J., Hintelmann, H., Feng, X. & Dimock, B. Unusual fractionation of both odd and even mercury isotopes in precipitation from Peterborough, ON, Canada. *Geochimica et. Cosmochimica Acta* **90**, 33–46 (2012).

83. Fu, X. et al. Mass-independent fractionation of even and odd mercury isotopes during atmospheric mercury redox reactions. *Environ. Sci. Technol.* **55**, 10164–10174 (2021).
84. Sherman, L. S. et al. Mass-independent fractionation of mercury isotopes in Arctic snow driven by sunlight. *Nat. Geosci.* **3**, 173–177 (2010).
85. Amos, H. M., Jacob, D. J., Streets, D. G. & Sunderland, E. M. Legacy impacts of all-time anthropogenic emissions on the global mercury cycle. *Glob. Biogeochemical Cycles* **27**, 410–421 (2013).
86. Sun, R. et al. Methylmercury produced in upper oceans accumulates in deep Mariana Trench fauna. *Nat. Commun.* **11**, 3389 (2020).
87. Motta, L. C. et al. Mercury isotopic evidence for the importance of particles as a source of mercury to marine organisms. *Proc. Natl Acad. Sci. Usa.* **119**, e2208183119 (2022).
88. MacSween, K. et al. Updated trends for atmospheric mercury in the Arctic: 1995–2018. *Sci. Total Environ.* **837**, 155802 (2022).
89. Ortiz, V. L., Mason, R. P. & Evan Ward, J. An examination of the factors influencing mercury and methylmercury particulate distributions, methylation and demethylation rates in laboratory-generated marine snow. *Mar. Chem.* **177**, 753–762 (2015).
90. Heyes, A., Mason, R. P., Kim, E.-H. & Sunderland, E. Mercury methylation in estuaries: Insights from using measuring rates using stable mercury isotopes. *Mar. Chem.* **102**, 134–147 (2006).
91. Lennon, J. & Pfaff, L. Source and supply of terrestrial organic matter affects aquatic microbial metabolism. *Aquat. Microb. Ecol.* **39**, 107–119 (2005).
92. Terhaar, J., Lauerwald, R., Regnier, P., Gruber, N. & Bopp, L. Around one third of current Arctic Ocean primary production sustained by rivers and coastal erosion. *Nat. Commun.* **12**, 169 (2021).
93. Schartup, A. T., Mason, R. P., Balcom, P. H., Hollweg, T. A. & Chen, C. Y. Methylmercury production in estuarine sediments: role of organic matter. *Environ. Sci. Technol.* **47**, 695–700 (2013).
94. Jiskra, M., Wiederhold, J. G., Bourdon, B. & Kretzschmar, R. Solution speciation controls mercury isotope fractionation of Hg(II) sorption to goethite. *Environ. Sci. Technol.* **46**, 6654–6662 (2012).
95. Lepak, R. F. et al. Factors affecting mercury stable isotopic distribution in piscivorous fish of the Laurentian Great Lakes. *Environ. Sci. Technol.* **52**, 2768–2776 (2018).
96. Bergquist, B. A. & Blum, J. D. Mass-dependent and -independent fractionation of Hg isotopes by photoreduction in aquatic systems. *Science* **318**, 417–420 (2007).
97. Kritee, K., Motta, L. C., Blum, J. D., Tsui, M. T.-K. & Reinfelder, J. R. Photomicrobial visible light-induced magnetic mass independent fractionation of mercury in a marine microalga. *ACS Earth Space Chem.* **2**, 432–440 (2018).
98. Kritee, K., Barkay, T. & Blum, J. D. Mass dependent stable isotope fractionation of mercury during mer mediated microbial degradation of monomethylmercury. *Geochimica et. Cosmochimica Acta* **73**, 1285–1296 (2009).
99. Madigan, D. J. et al. Mercury stable isotopes reveal influence of foraging depth on mercury concentrations and growth in Pacific Bluefin Tuna. *Environ. Sci. Technol.* **52**, 6256–6264 (2018).
100. Charette, M. A. et al. The transpolar drift as a source of riverine and shelf-derived trace elements to the central arctic ocean. *JGR Oceans* **125**, e2019JC015920 (2020).
101. Rodríguez-González, P. et al. Species-specific stable isotope fractionation of mercury during Hg(II) methylation by an Anaerobic Bacteria (*Desulfobulbus propionicus*) under Dark Conditions. *Environ. Sci. Technol.* **43**, 9183–9188 (2009).
102. Schartup, A. T., Soerensen, A. L. & Heimbürger-Boavida, L.-E. Influence of the arctic sea-ice regime shift on sea-ice methylated mercury trends. *Environ. Sci. Technol. Lett.* **7**, 708–713 (2020).
103. Baya, P. A., Gosselin, M., Lehnherr, I., St.Louis, V. L. & Hintelmann, H. Determination of monomethylmercury and dimethylmercury in the arctic marine boundary layer. *Environ. Sci. Technol.* **49**, 223–232 (2015).
104. St. Pierre et al. Importance of open marine waters to the enrichment of total mercury and monomethylmercury in Lichens in the Canadian High Arctic. *Environ. Sci. Technol.* **49**, 5930–5938 (2015).
105. Rosera, T. J. et al. Isolation of methylmercury using distillation and anion-exchange chromatography for isotopic analyses in natural matrices. *Anal. Bioanal. Chem.* **412**, 681–690 (2020).
106. *AVMA Guidelines for the Euthanasia of Animals: 2020 Edition*. (American Veterinary Medical Association, Schaumburg, IL, 2020).
107. Douglas, T. A. & Blum, J. D. Mercury isotopes reveal atmospheric gaseous mercury deposition directly to the arctic coastal snowpack. *Environ. Sci. Technol. Lett.* **6**, 235–242 (2019).
108. Blum, J. D. & Bergquist, B. A. Reporting of variations in the natural isotopic composition of mercury. *Anal. Bioanal. Chem.* **388**, 353–359 (2007).
109. GEBCO Compilation Group. GEBCO 2022 Grid. https://doi.org/10.5285/e0f0bb80-ab44-2739-e053-6c86abc0289c (2022).

Acknowledgements

We want to thank the captain and crew of RV Araon for excellent collaboration and support during the Arctic expedition ARA13B and C in 2022. This work was supported by Korea Institute of Marine Science & Technology Promotion (KIMST) funded by the Ministry of Oceans and Fisheries (Korea) [Grant number 20210541 (Air-sea exchange, sediment methylation, and ecosystem sources of mercury in the Arctic Ocean; S.K., S.H.), KIMST RS-2021-KS211500(Korea-Arctic Ocean Warming and Response of Ecosystem, KOPRI; E.Y.)] Also, this research was supported by a National Research Foundation of Korea Grant from the Korean Government (MIST; the Ministry of Science and (ICT) NRF-2021M1A5A1075513; S.K.) (KOPRI-NRF-2021M1A5A1075512.).

Author contributions

S.L. analyzed and interpreted the data and wrote the paper. S.K. and L.C.M. contributed to project ideas, sample planning, and data interpretation. S.K., E.Y., and S.H acquired the funding. S.L., Y.K., E.Y., T.R, J.H., S.H. performed fieldwork and/or managed the cruise. All authors contributed to the final data validation and feedback on writing.

Competing interests

The authors declare no competing interests.

Additional information

Supplementary information The online version contains supplementary material available at https://doi.org/10.1038/s41467-024-51852-2.

Correspondence and requests for materials should be addressed to Sae Yun Kwon.

Peer review information *Nature Communications* thanks the anonymous reviewers for their contribution to the peer review of this work. A peer review file is available.